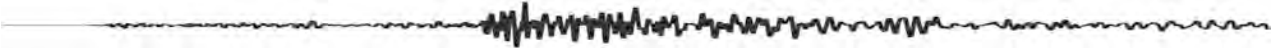




RÉSEAU ACCÉLÉROMÉTRIQUE PERMANENT
FRENCH ACCELEROMETRIC NETWORK



Programme de recherche 2015

Financé par le Ministère de l'Écologie, du Développement Durable et de l'Énergie

Dans le cadre des activités du GIS-RAP

RAPPORT FINAL

Study of in-situ nonlinear soil response in the French Antilles **γ -G Antilles**

Fabian Luis Bonilla¹, Diego Mercerat², Julie Régnier², Fernando Lopez-Caballero³, Philippe Guéguen¹

¹IFSTTAR, ²CEREMA, ³Ecole Central ParisTech

Prédiction de la réponse non linéaire des site en utilisant des données de forages. Application au site de belleplaine (Guadeloupe)

Rapport Final: Novembre 2016

Introduction

Les effets du site et leur réponse non linéaire sont généralement considérés comme un élément clé dans l'évaluation des risques sismiques. En effet, ils contrôlent la variabilité spatiale du mouvement du sol et la distribution des dommages pendant un tremblement de terre. Les coefficients associés aux conditions de site et à leur réponse non linéaire ont été introduits récemment dans les équations de prédiction du mouvement du sol (Abrahamson et al., 2014, Boore et al., 2014) et on constate que les incertitudes associées contribuent de façon significative aux incertitudes totales contenues dans ces équations, et par conséquent dans les études sur le risque sismique (Rodriguez-Marek et al., 2011, Bommer et Abrahamson, 2006). Il est couramment admis que les sédiments non consolidés ont tendance à réagir de manière non linéaire (par exemple, Field et al., 1997, Bonilla et al., 2005). Cependant, la réponse non linéaire du sol nécessite non seulement des reconnaissances géophysiques in situ pour caractériser les propriétés élastiques des matériaux, mais aussi des essais en laboratoire pour évaluer les paramètres décrivant leur comportement non linéaire.

En général, la réponse non linéaire des couches de sol est caractérisée par la dégradation du module de cisaillement G et l'augmentation de l'amortissement ζ à mesure que la déformation de cisaillement du sol augmente. En conséquence, la réponse non linéaire tend à réduire l'amplification haute fréquence du site, liée à l'augmentation de l'amortissement et au décalage de la fréquence de résonance du site vers des fréquences plus basses en raison de la diminution de la vitesse de cisaillement V_s (Dimitriu et al., 2002, Pavlenko et Irikura, 2002, Rubinstein et Beroza, 2004, 2005, Assimaki et al., 2008, Bonilla et al., 2005, et Régnier et al., 2013). G (et par conséquent V_s) et ζ sont généralement obtenus en utilisant des tests en laboratoire appliqués à des échantillons de sol recueillis sur le terrain tandis que la réponse des sites, y compris les effets non linéaires, est observée en utilisant des enregistrements de tremblements de terre. On peut alors s'attendre à des différences entre les tests de laboratoire et les observations de terrain en raison de la non reproductibilité de la pression de confinement in situ du sol en laboratoire, du remaniement des échantillons au moment du prélèvement, ou de la difficulté de séparer les effets non linéaires des effets d'amplification en lien par exemple avec les effets géométriques tridimensionnels (par exemple Frankel et al., 2002, Assimaki et al., 2008, Sleep, 2010).

Pour lever certaines ambiguïtés sur l'opposition effets de site *versus* effets non-linéaires, les données provenant de réseaux verticaux sont généralement utilisés (Frankel, 1999). Des méthodes existent pour évaluer la vitesse V_s le long d'un réseau vertical, basées sur les inter-corrélations des enregistrements entre chaque profondeur (Zeghal et al., 1995; Pavlenko et Irikura, 2003; Rubinstein et Beroza, 2004, 2005). Récemment, l'interférométrie sismique par des méthodes de déconvolution a été appliquée avec succès (Sawazaki et al., 2009, Nakata et Snieder, 2011, Mehta et al., 2007, Chandra et al 2015, 2016, Guéguen, 2016) pour évaluer la vitesse de cisaillement des ondes et leur variation en fonction des variations de contrainte ou de déformation. Cette méthode fournit une solution efficace pour obtenir les paramètres élastiques de la colonne du sol. De plus, elle a également été utilisée pour suivre la non-linéarité le long du profil de sol en relation avec

l'augmentation de la déformation (Chandra et al., 2015, 2016, Guéguen, 2016). La déformation était dans ces cas là calculée grâce à un proxy de déformation reliant la vitesse de cisaillement V_s à la vitesse maximale particulaire, c'est-à-dire le PGV. Cette déformation peut être calculée par PGV/V_s (Rathje et al. 2004). De plus, l'accélération de pic au sommet de la colonne de sol (PGA) est un proxy de la contrainte et le diagramme *PGA versus PGV/V_s*, voir *PGA versus PGV/V_s30*, peut être associé à une courbe contrainte-déformation, c'est-à-dire à un essai in-situ comparable aux essais de laboratoire (Idriss, 2011; Chandra et al., 2015, 2016). Guéguen (2016) a également proposé une mise à jour de la relation in-situ contrainte-déformation en considérant les spectres de réponse à la place du PGA.

Objectifs du projet

Dans ce projet, nous avons proposé un moyen d'exploiter les enregistrements de réseaux verticaux pour la prévision de la non-linéarité. Le site de Belleplaine aux Antilles a été considéré. Après la description du site, l'interférométrie sismique par déconvolution est appliquée aux données de séismes pour obtenir un profil de vitesse V_s comparé au profil de vitesse issu de reconnaissances géophysiques (Guéguen et al., 2011). La fonction de transfert (rapport des spectres de Fourier entre la surface et le fond de la colonne de sol), obtenue avec les données accélérométriques, est ensuite inversée pour obtenir un profil théorique du sol en considérant le profil expérimental comme la référence. Il est ensuite utilisé pour prédire numériquement la réponse non linéaire du site.

Résultats

La répartition des vitesses obtenues par interférométrie sismique permet de comprendre la variabilité en profondeur de la réponse du sol due aux ondes incidentes. Nous avons constaté que les quinze premiers mètres ne sont pas bien contraints par les données géophysiques ou par les données de forage, ce qui signifie que de fortes variations du modèle de sol peuvent exister à cette profondeur pour les différents séismes utilisés. Cela peut être dû à la présence d'une inversion de vitesse: le champ d'onde est ainsi assez complexe dans la partie plus rigide de la colonne de sol.

Une autre observation intéressante est l'atténuation remarquable du champ d'onde descendant (partie causale de la fonction de réponse impulsionnelle) que 'on obtient sur les interférogrammes sismiques. Les données expérimentales montrent une atténuation importante, que nous ne reproduisons pas avec les modèles élasto-plastiques utilisés dans la simulation. Le mouvement sismique incident à faible amplitude reste donc principalement élastique, c'est-à-dire sans atténuation significative dans les simulations. Une meilleure prise en compte numérique est donc nécessaire.

Dans tous les cas, la réponse observée au site de Belleplaine n'est pas facile à reproduire. Cela suggère que certains effets de propagation des ondes 2D ou 3D peuvent exister. Une fois les paramètres élastiques du site caractérisés par interférométrie sismique, avec leur incertitude, nous pouvons avancer dans la prédiction de la réponse non linéaire du sol. Pour cela, nous profitons des tests de laboratoire cycliques réalisés précédemment pour les deux types de sols présents sur le site. En l'absence de mouvements forts enregistrés jusqu'à présent, nous avons utilisé huit accélérogrammes enregistrés sur des sites rocheux et provenant d'une base de données mondiale. Nous observons que parmi les huit, six accélérogrammes développent des déformations de l'ordre de 10^{-4} : les fonctions de transfert associées sont assez proches de celle considérée comme élastique, c'est-à-dire sous faible déformation. Par contre, les deux accélérogrammes restant produisent des déformations plus grandes, générant un effet non linéaire visible sur la variation de vitesse en particulier. Une fois encore, l'utilisation de l'interférométrie sismique est utile pour analyser ces résultats parce que les fonctions impulsionnelles ainsi calculées montrent clairement l'atténuation de l'onde descendante pour ces deux accélérogrammes. De plus, les vitesses diminuent ce qui suggère

que la mangrove située entre -18 et -39m absorbe la majeure partie de la déformation, agissant comme un isolateur sismique de la couche de sol superficielle plus rigide, comme cela avait déjà été suggéré par Guéguen et al. (2011).

Conclusions

Grâce à cette étude, nous pouvons valider la relation contrainte-déformation expérimentale, c'est-à-dire PGA-PGV/Vs et au-delà PGV/Vs30. Cette conclusion nous laisse imaginer une évaluation in-situ de l'ensemble des stations du RAP, aux Antilles mais aussi ailleurs, pour tenter de proposer un proxy de déformation et pourquoi pas remonter à une évaluation de la non-linéarité in-situ.

Le paramètre de déformation PGV/Vs30, ou plus indirectement les paramètres liés au modèle hyperbolique classique relation contrainte et déformation, sont des paramètres qui pourraient avantageusement être introduits dans les modèles de prédiction du mouvement du sol, permettant d'identifier une source de l'incertitude épistémique liée à la déformation.

Prediction of non-linear site response using downhole array data and numerical modeling: the Belleplaine (Guadeloupe) case study

Luis Fabian Bonilla¹, Philippe Guéguen², Fernando Lopez-Caballero³, E. Diego Mercerat⁴,
Céline Gélis⁵

1. Université Paris Est, IFSTTAR, Marne-la-Vallée, Paris, France

2. ISTERre, CNRS/IFSTTAR, Université Grenoble–Alpes, France

3. Laboratory MSSMat CNRS UMR 8579, CentraleSupélec, Paris-Saclay University, Châtenay-Malabry, France

4. CEREMA, DTer Méditerranée, Laboratoire de Nice, France

5. IRSN/BERSSIN, Fontenay-aux-Roses, France

Submitted for publication in **Physics and Chemistry of the Earth**

Special Issue: **Advance in seismic site response: usual practices and innovative methods**

Contact Author

Philippe Guéguen

ISTerre

SOUG-C, BP 53

38041 Grenoble cedex 9

France

Philippe.gueguen@ujf-grenoble.fr

Running title: Non-linear site response using downhole array

Abstract

In this study, we analyze the acceleration time histories data at the Belleplaine (Guadeloupe, French West Indies) vertical array, recorded between 2008 and 2014, to evaluate the seismic response of sediments. First, we apply the seismic interferometry by deconvolution method to compute the in-situ shear wave velocity between the sensor at the surface and the two shallow sensors located at GL-15m and GL-39m depth. The efficiency of this method is discussed by studying the variability of the velocity profile obtained and comparing with the in-situ geophysical survey of the site. Computed strains between sensors remain very weak, lower than 10^{-5} , meaning that nonlinearities are not expected for these events. Moreover, the small dispersion of shear wave velocities values deduced from seismic interferometry may be related to the elastic behavior of the soil column. Furthermore, the transfer functions between each sensor combination are inverted to obtain a new velocity profile compatible with the geological knowledge of the site. The lag times calculated by seismic interferometry are then used to constrain random perturbations of the inverted velocity profile, allowing to study the variability of the 1D soil response. Finally, using strong motion events from a worldwide dataset, we numerically predict the nonlinear response of the site based on shear wave velocity variation and the strain proxy computed by the particle velocity versus shear wave velocity ratio. We conclude that seismic interferometry by deconvolution is a robust and accurate solution to help extracting the shear wave velocity profile and to monitor the soil nonlinear response. This technique can be used when strong earthquakes will be recorded at this experimental site in order to track and assess nonlinear effects in the soil column.

Keywords

Nonlinear site effects, seismic interferometry, vertical array, strain proxy, Guadeloupe

1. Introduction

Site effects and their nonlinear response are generally considered a key element in seismic hazard assessment, controlling the spatial variability of ground motion and the damage distribution during an earthquake. Coefficients related to the site condition and nonlinear response of sediments have been introduced into the so-called empirical ground motion prediction equations, GMPEs, (i.e. Abrahamson et al., 2014; Boore et al., 2014) and the uncertainties associated to these terms contribute significantly to the total uncertainties reported in these equations as well as in seismic hazard studies (Rodriguez-Marek et al., 2011; Bommer and Abrahamson, 2006). It is commonly assumed that unconsolidated sediments tend to respond in a nonlinear manner (e.g., Field et al., 1997; Bonilla et al., 2005). However, nonlinear soil response requires not only in-situ geophysical surveys to characterize the elastic material properties, but also laboratory tests to identify the parameters describing the nonlinear soil behavior.

Nonlinear response of sediments is usually characterized by the degradation of the shear modulus G and the increase in damping ζ as the soil shear strain γ increases. Consequently, nonlinear response tends to reduce site amplification at high frequencies related to the increase of damping and to the shift of the site resonance frequency toward lower frequencies due to the decrease in shear-wave velocity (Dimitriu et al., 2001; Frankel et al., 2002; Pavlenko and Irikura, 2002; Rubinstein and Beroza, 2004; 2005; Assimaki et al., 2008; Bonilla et al., 2005; Bonilla et al., 2011; Régnier et al., 2013). G and ζ are generally obtained using cyclic laboratory tests applied to soil samples collected in the field whilst the response of the sites, including nonlinear effects, is observed using in-situ earthquake ground motion records. In consequence, we may expect differences between laboratory tests and field observations because of the non-reproducibility of in-situ confining pressure of soil in laboratory tests, sample disturbance or the difficulty to separate nonlinear effects from site-amplification effects, including two-dimensional/three-dimensional geometric effects (e.g., Frankel et al., 2002; Assimaki et al., 2008; Sleep, 2010).

Vertical arrays of accelerometers are generally used to resolve the scattering versus nonlinearity problem (Frankel, 1999). Methods exist to assess V_s along a vertical borehole array based on cross correlation (Zeghal et al., 1995; Pavlenko and Irikura, 2003; Rubinstein and Beroza, 2004, 2005). Recently, seismic interferometry by deconvolution methods (Sawazaki et al., 2009; Nakata and Snieder, 2011; 2012; Mehta et al., 2007, Chandra et al. 2015, 2016; Guéguen, 2016) were applied to vertical arrays for assessing

shear wave velocity and their variation according to water content changes or strain increase. This method provides an accurate solution for the elastic conditions of the soil column, namely P- and S-wave travel times between couples of sensors. In addition, it has also been used for tracking nonlinearity along the soil profile related to seismic ground motion amplitude (Chandra et al., 2015, 2016; Guéguen, 2016). For nonlinearity assessment, strains along the profile can be computed as the relative displacement between sensors or by considering the ratio of peak ground velocity (*PGV*) and shear wave velocity V_s (i.e. PGV/V_s) as a strain proxy (Rathje et al., 2004). Furthermore, the peak-ground acceleration (*PGA*) versus PGV/V_{s30} has been proposed as the in-situ stress-strain relationship (Idriss, 2011; Chandra et al., 2015, 2016), where V_{s30} is the average shear wave velocity in the upper 30 m layers conventionally used in earthquake engineering. Recently, Guéguen (2016) proposed an update of the stress-strain in-situ relationship considering response spectra in place of *PGA*. Finally, each earthquake recording can be considered as a single in-situ cyclic test.

Because borehole strong ground motion is relatively scarce, therefore difficult to use for nonlinear characterization, in this manuscript we propose a way to exploit vertical array records for nonlinear prediction coupling experimental data and numerical modeling. After the description of the Belleplaine test site, seismic interferometry by deconvolution is applied to the borehole array to obtain an experimental shear-wave velocity profile between sensors compared with the reference soil profile defined by in-situ surveys (Guéguen et al., 2011). The transfer function (surface/downhole Fourier spectral ratio) using accelerometric data is then inverted to obtain a theoretical soil profile considering the experimental one as reference, and used in the last section to numerically predict the nonlinear response of the site.

2. The Belleplaine test site

The geotechnical vertical array at Belleplaine is located in the Guadeloupe Island (French West Indies) close to the Caribbean subduction zone (Fig. 1). Since December 2007, the network has been operated and maintained by the Institute for Earth Sciences (ISTerre) in the framework of the activities of the French Accelerometric Network (Péquegnat et al., 2008), with help from staff at the Guadeloupe Observatory of Volcanology and Seismology (OVSG). The vertical accelerometric network is composed of three synchronized triaxial accelerometers (Episensor, full scale +/-2g) located at the free surface (GL-0m), 15 m (GL-15m), and 39 m (GL-39m) depth, respectively. Extensive geotechnical and geophysical studies were performed (e.g. well drilling and laboratory

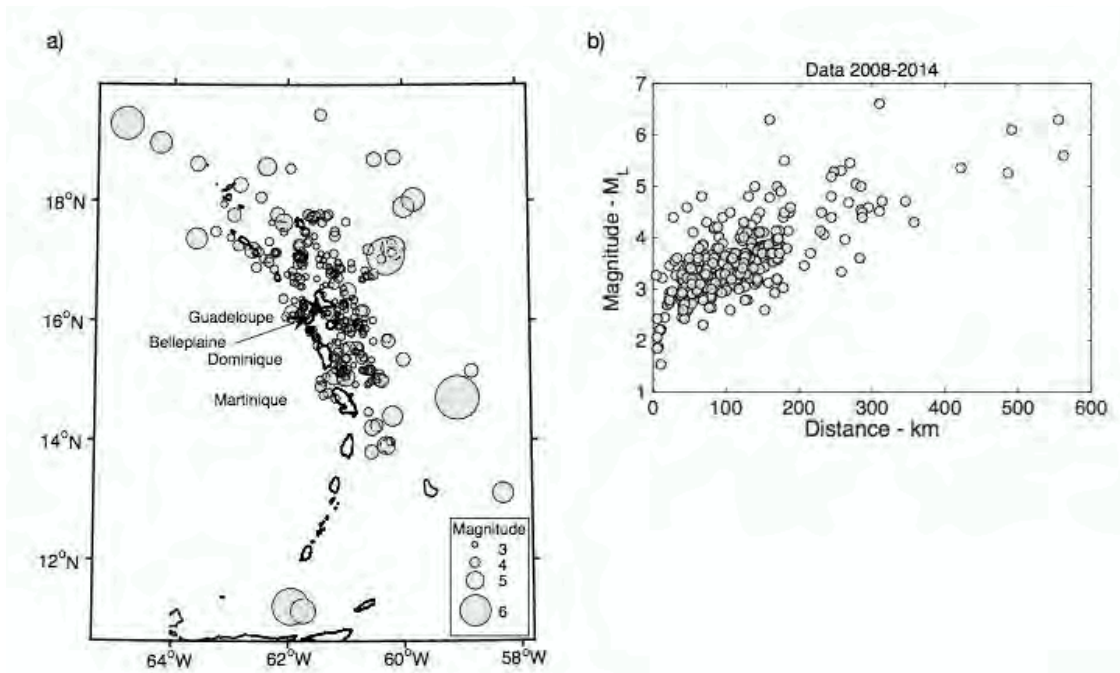


Figure 1: The Belleplaine test site. a) Localization of the site in the French West Indies (Caribbean sea) and localization of the earthquakes used in this study. b) Magnitude- distance distribution of the earthquakes

tests on samples, non-invasive seismic noise based methods, seismic piezocone) in order to define the soil profile. A synthesis of the soils characteristics is presented in Guéguen et al. (2011) by integrating all the information available and summarized in Tab. 1. After a 5-m-thick stiff shallow layer, a soft consolidated mangrove layer (33m thick) overlays the bedrock located at 38 m depth characterized by reef coral limestone. The S-wave velocity profile was estimated by manually fitting the amplitude of the transfer function between GL-39m and GL-0m sensors. In this configuration, GL-15m is located within the mangrove layer. Without additional information Q_s were roughly assumed equal to $V_s/10$ (Olsen et al., 2003).

Table 1 - Description of the soil profile of the Belleplaine site and obtained from geotechnical and geophysical surveys (after Guéguen et al., 2011).

Depth (m)	Description	Thickness (m)	V_s (m/s)	Q_s ($V_s/10$)
0-1m	Infills	1	200	20
1-5m	Stiffsand	4	470	47
5-38m	Mangrove	33	220	22
38-39m	Corallimestone	-	1500	150

Accelerometric data are continuously recorded using a 24-bit acquisition system at 125 samples per second and transmitted in real-time to the French national accelerometric data centre for archiving, storing and sharing (RAP-NDC). This data center is part of the

French national center for seismological data (RESIF-DC). The access to the data and the description of the instrumentation is available through the data select and station web-services developed by Federation of Digital Seismic Network (FDSN, <http://www.fdsn.org/>) and implemented at RESIF-DC (<http://www.resif.fr/>).

In this manuscript, only regional earthquake data were considered, extracted from continuous recording using the local magnitude epicenter catalogue provided by the Volcanological Observatory of Guadeloupe OVSG (Fig. 1a). In total, 296 earthquakes were recorded between 2008 and 2014, with magnitude between 1.5 and 6.6 and epicentral distance ranging between 1 and 300 km. Ambraseys et al. (2005) identified the engineering significance of earthquakes for $M_W > 5$ and a source-to-distance less than 150 km. Atkinson and Boore (2003) concluded that from a ground motion prediction point of view, nonlinearity of soil response is only important for recordings with peak ground acceleration (PGA) $> 100 \text{ cm/s}^2$. In our database, no data satisfying engineering criteria are available and PGA remains lower than 10 cm/s^2 . Nevertheless, soil nonlinearity is usually characterized as function of the strain of the soil. Based on laboratory tests, two different shear-strain thresholds related to soil nonlinearity are generally observed (Vucetic, 1994): linear cyclic γ_{tl} and volumetric γ_{tv} shear strains. Permanent deformation appears for strain larger than γ_{tv} , but nonlinear elastic behavior with negligible permanent deformation is often observed for strains values between γ_{tl} and γ_{tv} . The order of magnitude of γ_{tv} is around 10^{-4} (Hardin and Black, 1968; Drnevich and Richart, 1970; Dobry and Ladd, 1980). Johnson and Jia (2005) reported linear cyclic strains close to 10^{-6} and Chandra et al. (2015) and Guéguen (2016) observed degradation of shear wave velocity along vertical array for strains values around 10^{-5} . In Fig. 2, we observe an amplification of the ground motion between the bottom and the top of the vertical array, while there is no amplification between GL-15m and GL-0m on both horizontal components. This observation was previously analyzed by Guéguen et al. (2011) and they concluded on the equivalent base-isolation behavior of the soil column. Indeed, during an earthquake the soft mangrove layer plays the role of an isolating system for the uppermost stiff layer, minimizing amplification at high frequencies but also amplifying the motion at long periods, what can be detrimental for specific long period resonant structures. With this soil profile, the mangrove layer supports all the deformation of the soil column and the amplification is the largest in this layer. The relationship between nonlinear response and strain values will be analyzed in the rest of the manuscript.

3. Wave velocity determination using seismic interferometry

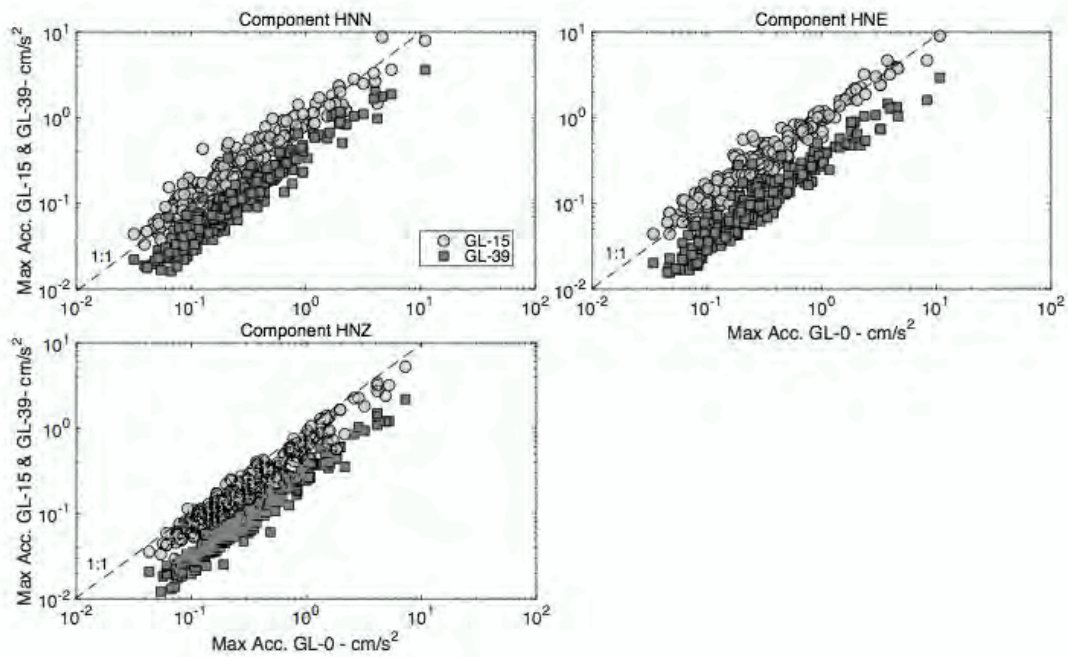


Figure 2: Distribution of the maximal acceleration recorded in the North-South (HNN), East-West (HNE) and Vertical (HNZ) at GL-0 compared to GL-15 and GL-39.

Seismic interferometry is a classical technique to estimate the Green's function between pair of receivers. It has been widely used in the past ten years for many different studies of site characterization (Pavlenko and Irikura, 2003, Mehta et al, 2009; Goudeard et al, 2008, Parolai et al 2009, Pilz et al 2012, Hanneman et al, 2014), monitoring oil and gas reservoirs (Bakulin and Calvert, 2006; Bakulin et al, 2007), structural identification of buildings (Snieder and Safak, 2006), monitoring of volcanoes (Wegler and SensSchoenfelder, 2006, Brenguier et al, 2008a, 2011) and fault zone studies (Rubinstein and Beroza, 2004, Brenguier et al., 2008b).

In the context of downhole seismic arrays, similar techniques have been applied since the seminal work of Elgamal et al, (1995) and Zeghal et al (1995), where signal cross-correlations were used to evaluate shear wave propagation characteristics and variations of shear wave velocity with respect to the level of input motion in the Lotung (Taiwan) downhole array. Haddadi and Kawakami (1998) and Kawakami and Haddadi (1998) developed the so-called Normalized Input–Output Minimization (NIOM) methodology to examine wave velocity variations using vertical array recordings. The technique has been applied to both the mainshock and the aftershocks of the 2007 Niigata earthquake at the Kashiwazaki-Kariwa nuclear site in Japan to assess shear wave velocity variations related to non-linear soil behavior in the first 100 m depth. The measured shear modulus reduction reaches values of 50% for shear strain levels around 10^{-3} (Mogi et al, 2010).

Mehta et al. (2007) use wavefield deconvolution to image near-surface properties for elastic media. Miyazawa et al (2008) applied seismic interferometry to extract P- and S-wave velocities, including shear wave splitting, from noise data recorded by downhole geophones at Cold Lake reservoir (Canada). Parolai et al (2009) analyzed earthquake data from the Atakoy accelerometric vertical array (Turkey) to obtain estimates of wave velocities. More recently, Nakata and Snieder (2011) used this technique to study the weakening of topmost layers in Japan after the Tohoku earthquake exploiting borehole data from the KiK-net network. They found values close to 5% - 10% of shear wave velocity reduction between 0-100 m depth before and after the earthquake. Nakata and Snieder (2012) compared results from cross-correlation and deconvolution interferometry of earthquake data recorded by KiK-net network, preferring the latter since the deconvolved signals are independent of the source power spectrum. More recently, Chandra et al (2015) and Guéguen (2016) studied non-linear soil behavior by seismic interferometry and several proxies for shear strain in the Garner Valley Downhole Array (California, US), the Wildlife Liquefaction Array (California, US) and Volvi test site (Greece).

In downhole array studies, the objective is the determination of local wave velocity profiles down to the deepest sensor in the array by picking the time delay of the deconvolved wave along the borehole. By choosing the reference sensor located at the ground surface (GL-0m), we estimate the time delay between up-going and down-going waves in the borehole from the delay times at the deconvolved signals at GL-15m and GL-39m. Then, under the assumption of vertical incidence of plane waves (assumption that can be too restrictive in case of 2D or 3D wave propagation effects), we directly obtain the shear wave velocity between pair of sensors by picking the lag-time of the maximum of the wave pulses in the horizontal components, respectively.

In this work, we calculate the deconvolved signals by seismic interferometry assuming the input and the output of the system as the recorded time histories at the bottom and top of the borehole and using the formula (Nakata and Snieder, 2011):

$$h(z, z_0, t) = FT^{-1} \left(\frac{U(z, \omega) * U(z_0, \omega)}{U(z_0, \omega)^2 + k * \max(U(z_0, \omega)^2)} \right) \quad (1)$$

where FT^{-1} denotes inverse Fourier transform, $U(z, \omega)$ and $U(z_0, \omega)$ the signals at z and at the surface, respectively and k the water level coefficient, that needs to be found experimentally as the smallest value producing stable deconvolved wavefields (i.e.

Chandra et al. 2014, 2015). After testing the slight influence of the k value, it was set at 10% of the maximum spectral power. Before deconvolution, the mean of the signal was removed and the signal de-trended. A 2nd-order Butterworth filter was applied between 0.5 and 15Hz where the maximum energy is present in the accelerometric data and large enough to have an accurate picking of the pulse in the time-domain. The inverse Fourier Transform is applied to $H(z_i, z_0, \omega)$ (Eq. 1) to obtain the impulse response of the soil column between sensors $GL-i$ and $GL-0$. We resampled 10 times the impulse response using a polyphase antialiasing filter to resample the signal at a uniform sample rate and to improve the accuracy of travel time picking. The pick of the up-going (non-causal) pulse was then manually selected for all signals. Only the horizontal components (HNE and HNN) were taken into account since the soil column is considered as a system in shear deformation. The mean shear wave velocity between two sensors was computed by dividing the depth of each sensor by the pulse travel time.

Figure 3 shows the deconvolved signals with respect to $GL-0$ and the picked travel time delay or lag time of the pulse propagating along the vertical array for all the events selected. Time delays are observed between $GL-0$ and $GL-15$, and $GL-15$ and $GL-39$, and $GL-0$ and $GL-39$ pair of sensors. We note that the pulse is not clearly observed along the profile, as consequence of the small events recorded and the possible high attenuation at the Belleplaine site. The travel time picks on the average curves (red lines in Fig. 3) gives an average V_s value of 211 m/s, 160 m/s and 174 m/s between $GL-0$ and $GL-15$, $GL-15$ and $GL-39$, and $GL-0$ and $GL-39$, respectively. The order of magnitude is very similar to the original shear wave velocity profile presented in Guéguen et al. (2011). In Fig. 4, we display the variation of V_s with respect to the deformation computed as the relative displacement between sensors. Before computing the displacement, we applied Boore's (2005) recommendation for processing accelerometric data, which transforms the signals to obtain the same length, by applying zero padding before filtering and integration. Velocities obtained by deconvolution are quite stable and the variation of the estimate is quite limited, with coefficient of variation (σ/μ) equal to 11%, 4% and 15% for 0-15m, 0-39m and 15-39m inter-sensor distances, respectively. We note a constant value of V_s for larger strains and a greater dispersion for small events, corresponding to small strain values, as a consequence of the low signal-to-noise ratio in the frequency domain computed when selecting the data between the pre-event noise and the earthquake data windows. However, the strain remains very weak, lower than 10^{-5} , i.e. nonlinearities are not expected for these events. The small dispersion of V_s values suggests the high

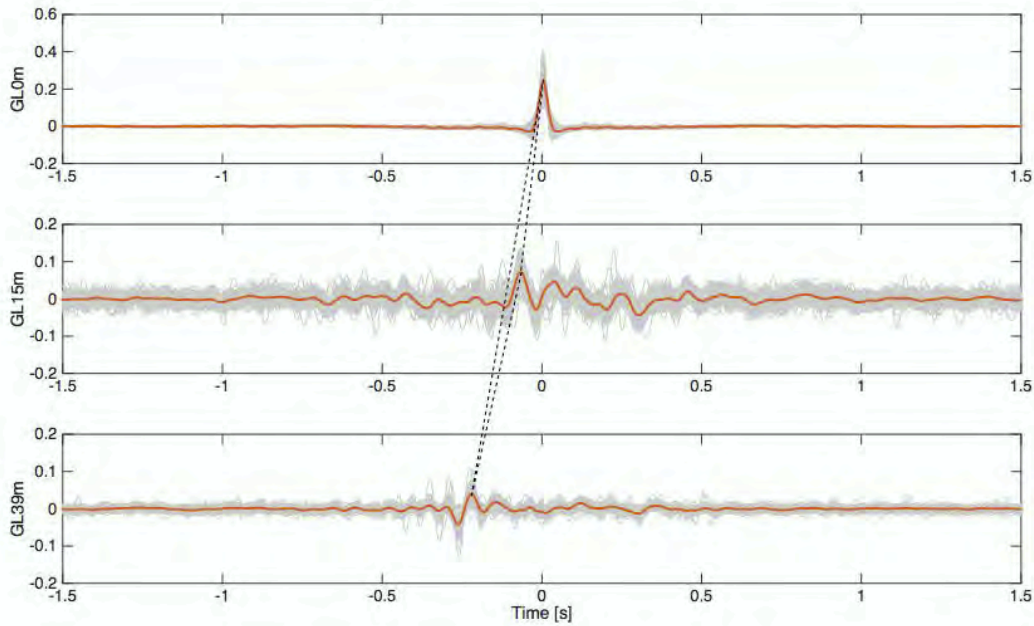


Figure 3: Seismic interferometry by deconvolution results. Gray line is for each event and red line corresponds to the mean impulse response. Dashed lines are the time lag picking used for computing the shear waves velocity.

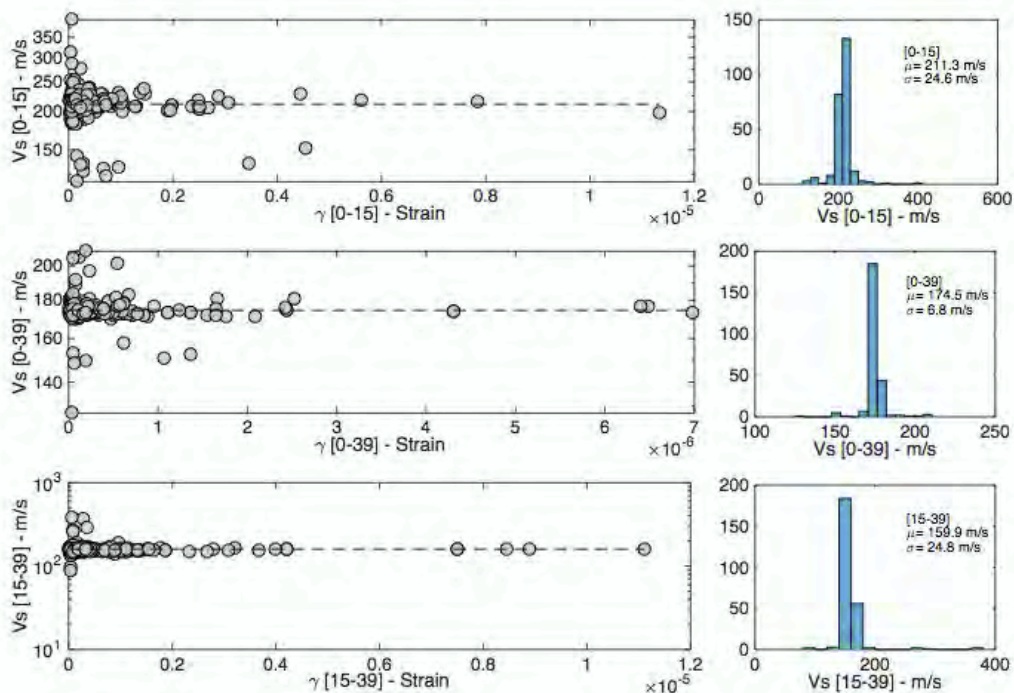


Figure 4 - Shear wave velocity computed by deconvolution between GL-0 and GL-15, GL0 and GL39 and GL15 and GL39. Each dot corresponds to one earthquake recorded at Belleplaine test site, the dashed line is the average shear wave velocity of the results, σ and μ mean the mean value and the standard deviation of the shear waves velocity. Note that the scale on x-axis is not the same.

accuracy and robustness of the seismic interferometry by deconvolution method for in-situ shear wave velocity analysis when determining the elastic properties of the soil column, a step needed before going to any numerical prediction of nonlinear response.

4. Determination of elastic soil properties

In the previous section, seismic interferometry was used to estimate the travel time between two sensors and then to derive an approximate velocity profile for the Belleplaine site. The computed travel times confirm the presence of stiff material in the first 15 m and softer soil in the last 24 m depth. These travel times agree with the stratigraphic description in Guéguen et al. (2011). In order to better characterize the site, we invert the observed mean transfer function, in the frequency band of 0.5 to 10 Hz, between the surface and 39 m depth to obtain the soil profile, i.e. the shear wave velocity and attenuation factors Q_s , using a hybrid global search algorithm that combines simulated annealing and downhill simplex methods (Liu et al., 1995) for vertically incident SH waves and borehole boundary conditions following the Haskell-Thomson method (Haskell, 1953; Thomson, 1950). The transfer function is the Fourier spectral ratio between the surface and downhole records. Observed transfer functions are computed using the whole record. Each acceleration time history has the mean removed, and a taper of 2.5% Hanning window is applied before computing the Fourier transform. Signal-to-noise ratio greater than three is assured. Noise is approximated by at least 10 s of pre-event noise. A Konno-Ohmachi smoothing with a bandwidth of 40 (Konno and Ohmachi, 1998) is used prior computing the spectral ratios. Finally, the geometric mean of transfer functions is computed.

For the inversion procedure, the a priori information is obtained from Guéguen et al. (2011), considered as our reference model. In particular, we keep the density values from Guéguen et al. (2011) and since we have some information about the stratigraphy of the soil column, we allow a small perturbation on the layer thickness. In order to test the homogeneity of the mangrove an extra layer is added in this geological layer. Gueguen et al. (2011) found the velocity at GL-38m to be 1500 m/s to match the observed transfer function. There is no geophysical exploration up to this depth. Thus, we also explore this bedrock velocity. For this reason we end up with six layers instead of the original four shown in Table 1. Finally, the values that were allowed to fully vary in the global search algorithm are the ones corresponding to the shear velocity and Q_s , respectively. The resulting “best” profile is shown in Table 2.

Table 2: Soil profile extracted from inversion using the mean transfer function between 0 m and 39 m depth.

Depth (m)	Density (kg/m ³)	Thickness (m)	Vs (m/s)	Qs
0-3.90	1900	3.90	400	32
3.90-4.84	1600	0.94	195	44
4.84-9.68	1600	4.84	333	19
9.68-13.68	1600	5.00	245	46
13.68-37.10	1600	23.42	205	18
37.10-38.0	2200	0.98	1468	148

The resulting soil model predicts slight differences in the theoretical travel times calculated from Table 2 with respect to the ones obtained with seismic interferometry. Thompson et al. (2009) show the importance of incorporating spatially correlated variability of the seismic properties to fit observed transfer functions using Kik-Net stations pairs located at depth and at the surface. In order to assess the effect of soil properties variability on the site response, we compute ten thousands random profiles around the one shown in Table 2 following the Rathje et al. (2010) procedure to perform a random perturbation around the mean model using spatial correlation. Furthermore, we select 200 models producing travel times that are within the observed in-situ variability.

Figure 5 (left) shows the set of models (i.e., random velocity profiles) that satisfy the constraints of the inversion, i.e. by using the lag-times issued from seismic interferometry. We can see that the first 15 m are not well constrained and multiple combinations could explain the observed travel time. This is not the case for the deeper mangrove material between GL-15 and GL-39; however, the predicted travel time is slightly higher than the observed one. Figure 5 (right) shows the observed (mean value), initial theoretical, and random transfer functions. We can see that the main amplification peaks are relatively well explained by the model, but the match of their amplitude remains a difficult task. Indeed, the travel time variability is translated into transfer functions that have frequency peaks slightly shifted to the left. Another issue is the observed broadband amplification between 4 and 10 Hz. Only the peak locations have been reproduced, having an overall similar attenuation. For these reasons we do not know whether this site is a perfectly 1D-site or whether frequency dependent Qs values may better explain the observations (e.g. De Martin et al., 2013; Satoh et al., 1995; Satoh, 2006). These possibilities are out of scope of this work and will be subject of further research. In any case, the use of seismic interferometry greatly helped to constrain random velocity profiles when selecting compatible models with observed soil amplifications.

5. Nonlinear site response

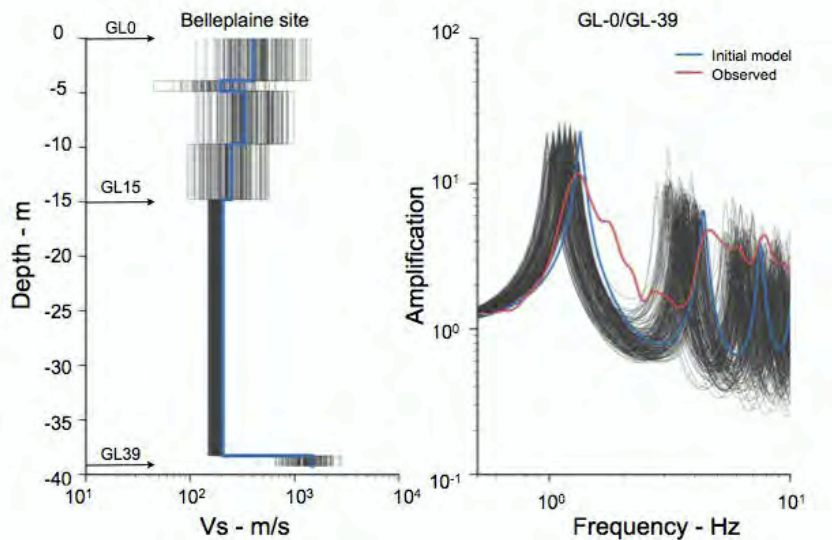


Figure 5: Left: initial velocity profile (blue) and random velocity profiles (black). Arrows indicate the depth of the sensors. Right: observed transfer function between 0 and 39 m depth (red), initial theoretical transfer function (blue), random transfer functions (black).

Because of the lack of strong ground motion data for the Belleplaine site, we carry out 1D numerical simulations of wave propagation. We used the results of the previous section including non-linear soil parameters from laboratory tests and from bibliography for the other layers.

5.1 Numerical method and nonlinear soil model

A layered soil/rock model is considered. The soil profile is composed principally of clay, sandy (i.e. D_r 60%) and mudflats soils. The total thickness of site profile is 39 m. The numerical model is based on the site profile given Tab. 2. The elastoplastic model implemented in *CyberQuake* (Modaressi and Foerster, 2000) is used to represent the soil behavior. The cyclic *CyberQuake* model is written for laterally infinite parallel soil layers, where a one-dimensional geometry can be considered. Concerning the bedrock's boundary condition, as the signal recorded at the sensor placed at GL-39m consists of an incoming wave plus its reflection from the free surface, and in order to provide a compatibility of displacements between the simulated by the numerical model and the recorded signal at the borehole sensor, a boundary condition inspired by the Domain Reduction Model (Bielak et al., 2003) was used. It consists to impose the recorded waves at the base of the model as effective forces and to use absorbing boundary only to satisfy a radiation condition for the incompatible outgoing waves.

The water level is placed at 2 m depth. Regarding the elastoplastic model, it can take into account the soil behavior in a large range of strains and is written in terms of effective

stress. The representation of all irreversible phenomena is made by deviatoric plastic deformation mechanisms and incorporates dilatancy-contractance in the normal direction to that plane. The model uses a Coulomb type failure criterion and the critical state concept. The evolution of hardening is based on the plastic strain (i.e. deviatoric and volumetric strain). To take into account the cyclic behavior, a kinematical hardening based on state variables at the last load reversal is used. The soil behavior is decomposed into pseudo-elastic, hysteretic and mobilized domains. See Modaressi and Foerster (2000) and Lopez-Caballero et al. (2007) and references therein for further details about the model. The parameters of the model concern both the elastic and plastic behavior of the soil. The elastic model parameters (i.e. V_s and V_p) for each layer are summarized in Tab. 2 and the other soil parameters were determined with the procedure defined by Lopez-Caballero et al. (2007). Figure 6 shows the model prediction for the variation of shear modulus ratio (G/G_{max}) and damping (D) with the cyclic shear strain (γ) for both sand and mudflats. The modeled test results (dashed lines) for the mudflats soils are compared to the measured ones (dots) in a resonant column test (RC). The other soil layers have similar curves and are not shown here for the sake of brevity. It is noted that for the mudflats, the obtained shear degradation curve ($G/G_{max}-\gamma$) match relatively good, on the contrary for the damping (D), it can be seen an underestimation for strains less than 10^{-5} . Elastoplastic constitutive models, as the one used in this analysis, require the addition of a small amount of low strain damping to avoid spurious response at very low strain levels. The numerical algorithm of the dynamic equilibrium solution in the time domain introduces this damping (Montoya-Noguera and Lopez-Caballero, 2016). In this case, the numerical damping “added” into the model is 0.1 % and is applicable for strains less than 10^{-4} . These simulations allow verifying the coherence of the nonlinear model parameters for the computations, which will be performed in section 5.3

5.2 Response of the synthetic ground motion at Belleplaine

In order to assess the effect of the input motion on the site response and the relevancy of the strain proxy, we used 60 recordings of 2014 to carry out the wave propagation in the Belleplaine site model. Figure 7a shows the transfer functions calculated between different sensors. In red, we have the observed soil amplifications and in black and grey the mean and the 99% confidence limits of the synthetic transfer functions, respectively. We can clearly see that practically there is no variability in the computed site response as a function of the input ground motion level. Assuming that the

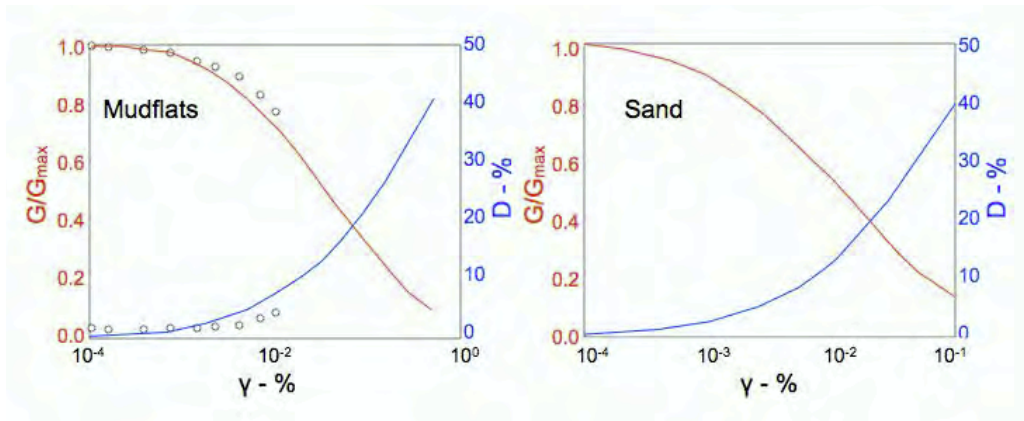


Figure 6 - Simulated G/G_{\max} - γ and D - γ curves for a) Mudflats model and b) Sand model. Open circles correspond to the RC test for mudflats.

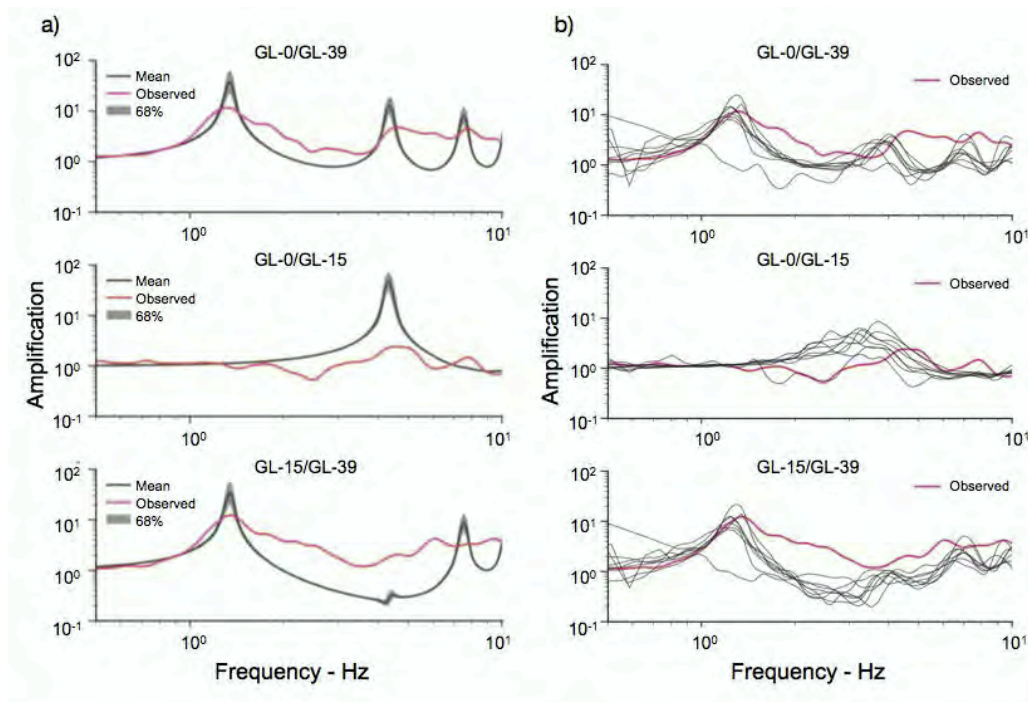


Figure 7: (a) Observed (red) and computed (black) transfer functions for nonlinear wave propagation of recorded signals in 2014. The 68% confidence limits are shown in gray. (b) Observed (red) and computed transfer functions for eight strong motion signals from PEER database (gray).

material of the soil profile is well characterized as well as the nonlinear properties, this numerical soil transfer functions confirm that the recorded ground motions represent mainly the linear behavior of the soil column, as also observed Fig. 4 for constant V_s values obtained by seismic interferometry by deconvolution. This is consistent with small strain levels deduced from recordings (Fig. 4).

Figure 8 shows the mean impulse response function (Eq. 1) using these synthetics. The reference for the deconvolution is always the topmost sensor, either GL-0 or GL-15. Thus, the up-going and down-going waves can be seen in the non-causal and causal parts

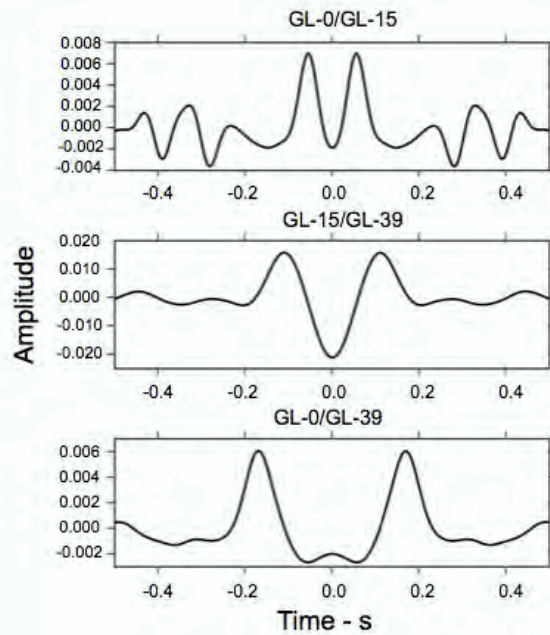


Figure 8: Mean computed impulse response for the combination of the three sensors at Belleplaine.

of the impulse response function, respectively. Since the nonlinear model is an elastoplastic rheology, which does not allow hysteretic damping at low strains, and despite the numerical damping introduced, we can observe that there is no much attenuation in the reflected wave (down-going wave field in the positive time values). This also confirms that the recorded ground motion does not trigger significant nonlinear material behavior, at least with the proposed velocity profile and the nonlinear material properties as it has also been observed by Chandra et al. (2016) modeling centrifuge tests.

5.3 Predicting nonlinear soil behavior at Belleplaine

In the absence of recorded strong motion at the site, we used eight signals from the Pacific Earthquake Engineering Research Center (PEER) database to study the nonlinear soil response at the Belleplaine site. The events range in magnitude between 5 and 6 and the recordings are at site-to-source distances from 5 to 50 km and dense-to-firm soil conditions (i.e. $600\text{m/s} < V_{s30} < 800\text{m/s}$). The characteristics of the input ground motions are listed in Table 3 and Figure 7b shows the computed transfer functions for the three combinations of sensors. We observe more dispersion on the soil amplification curves than in the case of weak input motion. This dispersion comes from the variability of the nonlinearity response with respect to the input ground motion. Furthermore, there is a clear de-amplification at high frequencies compared to the mean observed transfer function (in red). Yet, the shift of the fundamental frequency is quite small.

Table 3 - Selected Ground motion records from NGA database (NGA# is the record sequence number at NGA database - <http://ngawest2.berkeley.edu/> - Rjb is the Joyner-Boore source-to-site distance)

NGA#	Event	Year	Station	Mag	Rjb (km)	PGA (g)	PGV (cm/s)	Vs30 (m/s)
23	San Francisco	1957	GoldenGatepark	5.28	11.0	0.09	391	874
43	Lytle Creek	1970	Cder Springs-Allen Ranch	5.33	16.7	0.06	147	813.5
45	Lytle Creek	1970	Devils Canyon	5.33	17.9	0.14	408	684.9
49	Lytle Creek	1970	Santa Anita Dam	5.33	42.4	0.04	133	684.9
106	Orovill-01	1975	OrovilleSeismograph station	5.89	7.8	0.08	371	622.9
133	Friuli-Italy-02	1976	San Rocco	5.91	14.4	0.06	544	659.6
150	Coyote Lake	1979	GilroyArray #6	5.74		0.43	4710	663.3
222	Livermore-02	1980	Livermore Morgan Terr Park	5.40	7.5	0.20	1096	712.8

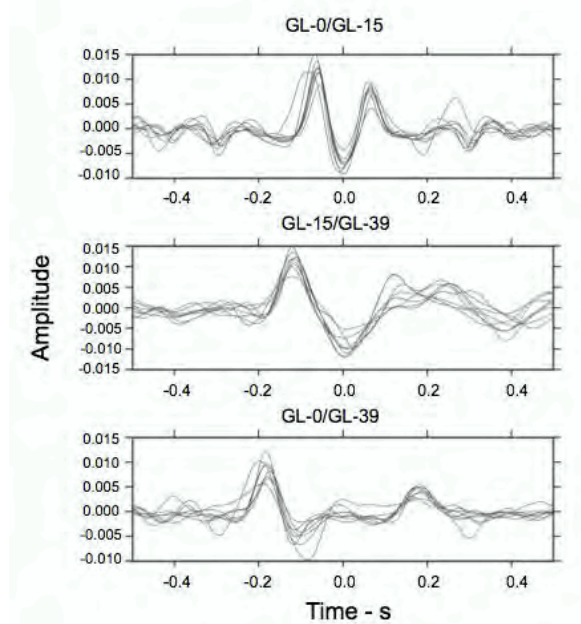


Figure 9: Impulse response functions for nonlinear wave propagation using the eight strong motion records from the PEER database (Table 3)

Figure 9 shows the impulse response functions for the computed motion using the strong motion PEER data. As it was previously mentioned, the reference station is the topmost sensor for each deconvolution pair. In this case, we can see that the down-going waves (causal) are attenuated due to the triggering of nonlinear soil behavior. In addition, the non-causal part of the impulse response function (negative time values) shows some dispersion that may be related to the Belleplaine's non-linear response of the site and particularly to the complex interaction between the input motion and the soil column properties, including nonlinear ones. Indeed, as shown by Gélis and Bonilla (2012) for one

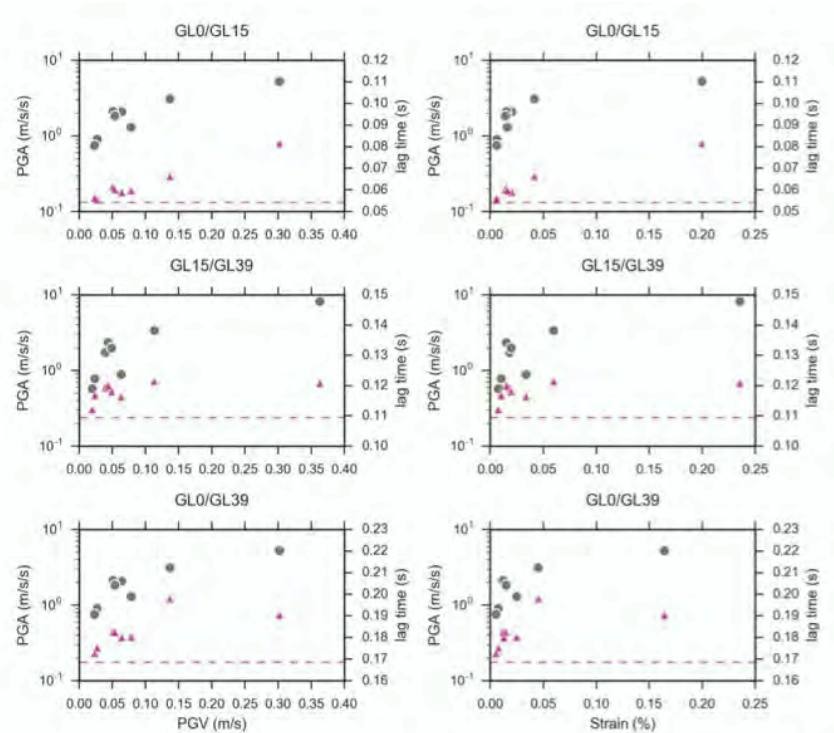


Figure 10: PGA vs PGV (left) and strain (right) (gray circles) together with lag times vs PGV and strain (red triangles) values for the eight nonlinear simulations using records from the PEER database. The red dashed line indicates the theoretical lag time for the linear model.

simple impulse-like and one realistic input motion, both sharing the same PGA, the input motion complexity and frequency content have a strong influence on the soil response and on the minimum shear wave velocity reached during wave propagation.

Figure 10 shows the PGA vs PGV and PGA vs strain as proxies for the stress-strain space (gray circles) for all three sensors. In addition, the estimated lag times for the strong motion inputs are also shown (red triangles). The red dashed line shows the theoretical linear travel time between the sensor pairs. One clearly sees that for strains less than $2.5 \cdot 10^{-4}$, the lag times are quite close to the linear estimate. However, when the ground motion increases, there are two PEER signals that trigger some nonlinear material behavior. Indeed, their PGV and strain values become large and the associated lag time visibly increases, indicating a reduction of the wave speed in the medium. Furthermore, larger deformations and longer lag times are noticed for the couple GL-15 – GL-39 sensors. This suggests that nonlinear behavior is stronger in the last 24 m depth of the soil column, where most of the incoming wavefield remains trapped. This agrees with Guéguen et al. (2011) results that suggest that the mangrove acts as a seismic isolator system and it takes most of the deformation of the soil column. Note that these results are based on a couple of simulations only, thus more analyses should be done and more importantly,

more records of strong motion are needed in this site to understand wave propagation in the mangrove and its seismic isolation characteristics.

6. Discussion and Conclusions

Belleplaine downhole array is located in the French West Indies, the most seismically active area of France, where large subduction earthquakes are expected. Though, this site has not yet recorded strong motions, making difficult to empirically study nonlinear soil response of the soil column. However, it is possible to take advantage of the recorded weak motion seismicity to assess its linear response. This is very important and it should be systematically done before conducting any nonlinear soil response study in order to separate nonlinear material behavior from other phenomena related to an unknown or poor velocity model characterization.

To do that, we use the traditional Fourier spectral ratios to assess linear transfer function between different sensors pairs. The soil amplification between the surface and GL-39 m is then used to invert the velocity and Q_s values. To better constrain the solution we use a priori information from previous studies (i.e. Guéguen et al., 2011). Furthermore, the originality of this study lies on the use of seismic interferometry by deconvolution to obtain the travel time of S-waves between the sensor pairs. In this case, it is possible to have travel times estimates as well as deformations for each recorded event. This additional information allows assessing the strain dependency of the recorded ground motion. Therefore, the knowledge of deformation inside of the soil column is critical if we want to know whether the soil deforms in elastic or nonlinear regime to compare to existing laboratory tests. In addition, since we have the deformation and associated travel time we can estimate an empirical in-situ shear modulus curve (Chandra et al., 2015, 2016; Guéguen, 2016).

The travel time distribution also provides insight of the intrinsic variability of the soil response due to the incoming waves such as the amplitude and incident angle. Moreover, it permits constraining random soil models that may explain equally well the observations. Indeed, we use them to explore the random response of Belleplaine site and we found that the upper 15 m are not well constrained. This means that some strong variations of the soil model may exist at this depth. This might be because there is a velocity inversion from low velocities below this interface to higher values close to the surface. Thus, the wavefield is relatively complex in the stiffer part of the soil column. This is also seen in the mean impulse response between GL-0m and GL-15m (Figures 3 and 8), where there is a presence of stronger oscillations compared to the results between GL-0m and GL-39m or

GL-15m and GL-39m. Another interesting observation is the remarkable attenuation of the downgoing wavefield (causal portion of the impulse response function). Empirical data show some attenuation, but the synthetic does not. The latter is probably due to the elasto-plastic soil model used in the simulation. Low amplitude input motion remains mainly elastic, then there is no attenuation due to the absence of hysteretic behavior. This can be improved with a better implementation of small strain attenuation in the Finite Element code.

In any case, the observed response at Belleplaine site is not easy to replicate. This suggests that some 2D or 3D wave propagation effects may exist, something that we need to further study to better assess seismic hazard at this site.

Once the elastic parameters of the site have been characterized, together with their uncertainties, we could move forward predicting nonlinear soil response. We take advantage of the cyclic laboratory tests for the two kinds of soils present at the site. In the absence of strong motion, we used eight acceleration time histories recorded at rock sites from a known worldwide database to propagate them through the soil column. We observe that six time histories develop strains close to 10^{-4} , whose transfer functions are quite close to the linear estimate. Two accelerations produce larger strains mobilizing some visible nonlinear effect. Once again, the use of seismic interferometry is helpful to analyze these results because the computed impulse response functions clearly show the attenuation of the down going wave for the stronger ground motion. Furthermore, the compute lag times also increase indicating a reduction of the velocity in the soil. These elements suggests that the mangrove absorbs most of the deformation acting as a seismic isolator for the overlaying stiffer soil as has already been postulated by Guéguen et al. (2011). However, such a system may amplify the motion at long periods, what can be detrimental for specific long period resonant structures. Yet, more numerical analyses should be done and more importantly recorded strong motion data will help to understand the behavior of the mangrove.

7. Acknowledgement

The authors would like to gratefully thank the French Accelerometric Network (RAP, <http://www.rap.resif.fr>) for supporting this work in the framework of the γ -G working group. Data are provided by the RESIF network through its web portal (RESIF-RAP French Accelerometric Network. RESIF - Réseau Sismologique et géodésique Français. Seismic Network. doi:10.15778/RESIF.RA <http://data.datacite.org/10.15778/RESIF.RA>).

8. References

- Abrahamson, N. A., Silva, W. J., Kamai, R., 2014. Summary of the ASK14 ground motion relation for active crustal regions. *Earthquake Spectra*. 30(3), 1025–1055.
- Ambrasey, N.N., Douglas, J., Sarma, S.K., Smit, P.M., 2005. Equations for the estimation of strong ground motions from shallow crustal earthquakes using data from Europe and the Middle East: horizontal peak ground acceleration and spectral acceleration. *Bulletin of Earthquake Engineering*. 3, 1–53.
- Assimaki, D., Li, W., Steidl, J.H., Tsuda, K., 2008. Site amplification and attenuation via downhole array seismogram inversion: A comparative Study of the 2003 Miyagi - Oki Aftershock Sequence. *Bulletin of the Seismological Society of America*. 98(1), 301-330.
- Atkinson, G.M., Boore, D.M., 2003. Empirical ground-motion relations for subduction-zone earthquakes and their application to Cascadia and other regions. *Bulletin of the Seismological Society of America*. 93(4), 1703-1729.
- Bakulin, A., Calvert, R., 2006. The virtual source method: Theory and case study. *Geophysics*. 71(4), SI139-SI150.
- Bakulin, A., Mateeva, A., Mehta, K., Jorgensen, P., Ferrandis, J., Herhold, I. S., Lopez, J. 2007. Virtual source applications to imaging and reservoir monitoring. *The Leading Edge*. 26(6), 732-740.
- Bielak, J., Loukakis, K., Hisada, Y., Yoshimura, C. 2003. Domain reduction method for three-dimensional earthquake modeling in localized regions, part I: Theory. *Bulletin of the Seismological Society of America*. 93(2):817–824,
- Bonilla, L.F., Archuleta, R.J., Lavallée, D., 2005. Hysteretic and dilatant behavior of cohesionless soils and their effects on nonlinear site response: Field data observations and modeling. *Bulletin of the Seismological Society of America*. 95(6), 2373-2395.
- Bonilla, L.F., Tsuda, K., Pulido, N., Regnier, J, Laurendeau, A., 2011. Nonlinear Site Response Evidence of K-Net and KiK-net Records from the 2011 off the Pacific coast of Tohoku Earthquake. *Earth Planets Space*. 63, 785-789.
- Boore, D.M., 2005. On Pads and Filters: Processing Strong-Motion Data. *Bulletin of the Seismological Society of America*. 95(2): 745–750 (2005).

- Boore, D.M., Stewart, J.P., Seyhan, E., Atkinson, G.M., 2014. NGA-West2 equations for predicting PGA, PGV, and 5% damped PSA for shallow crustal earthquakes. *Earthquake Spectra*. 30(3), 1057–1085.
- Bommer, J.J., Abrahamson, N.A., 2006. Why do modern probabilistic seismic-hazard analyses often lead to increased hazard estimates?. *Bulletin of the Seismological Society of America*. 96(6), 1967-1977.
- Brenguier, F., Shapiro, N.M., Campillo, M., Ferrazzini, V., Duputel, Z., Coutant, O., Nercessian, A., 2008a. Towards forecasting volcanic eruptions using seismic noise. *Nature Geoscience*. 1(2), 126-130.
- Brenguier, F., Campillo, M., Hadziioannou, C., Shapiro, N. M., Nadeau, R.M., Larose, E. 2008b. Postseismic relaxation along the San Andreas fault at Parkfield from continuous seismological observations. *Science*. 321(5895), 1478-1481.
- Brenguier, F., Clarke, D., Aoki, Y., Shapiro, N. M., Campillo, M., Ferrazzini, V., 2011. Monitoring volcanoes using seismic noise correlations. *Comptes Rendus Geoscience*. 343(8), 633-638.
- Chandra, J., Guéguen, P., Steidl, J.H., Bonilla, L.F., 2015. In-situ assessment of the G- γ curve for characterizing the nonlinear response of soil: Application to the Garner Valley Downhole Array(GVDA) and the Wildlife Liquefaction Array (WLA). *Bulletin of Seismological Society of America*. 105(2A), 993-1010.
- Chandra J., Guéguen P., Bonilla F., 2016. On the use of the seismic interferometry technique for testing PGV/Vs as a proxy for predicting nonlinear soil response. *Soil Dynamics and Earthquake Engineering*. 85, 146-160.
- De Martin, F., Matsushima, S., Kawase, H. 2013. Impact of geometric effects on near-surface Green's functions. *Bulletin of the Seismological Society of America*. 10(6), 3289-3304. doi:10.1785/0120130039
- Dimitriu, P., Theodulidis, N., Hatzidimitriou, P, Anastasiadis, A., 2001. Sediment nonlinearity and attenuation of seismic waves; A study of accelerograms from Mefkas, Western Greece. *Soil Dynamics and Earthquake Engineering*. 21, 63-73.
- Dobry, R., Ladd, R., 1980. Discussion of 'Soil liquefaction and cyclic mobility evaluation for level ground during earthquakes,' by H.B. Seed and 'Liquefaction potential: science versus practice,' by R. B. Peck. *Journal of the Geotechnical Engineering Division*. 106(6), 720-724.

- Drnevich, V.P., Richart, F.E., 1970. Dynamic prestraining of dry sand. *Journal of Soil Mechanics and Foundations Division*. 96(2), 453-469.
- Elgamal, A.W., Zeghal, M., Tang, H.T., Stepp, J. C., 1995. Lotung downhole array. I: Evaluation of site dynamic properties. *Journal of Geotechnical Engineering*. 121(4), 350-362.
- Field, E.H., Johnson, P.A., Beresnev, I., Zeng, Y., 1997. Nonlinear ground-motion amplification by sediments during the 1994 Northridge earthquake. *Nature*. 390, 599-602.
- Frankel, D.A., 1999. How does the ground shake ?. *Science*. 283(5410), 2032-2033
- Frankel, A.D., Carver, D.L., Williams, R.A., 2002. Nonlinear and linear site response and basin effects in seattle for the M 6,8 Nisqually, Washington, Earthquake. *Bulletin of the Seismological Society of America*. 92(6), 2090-2109.
- Gélis C. and Bonilla L.F., 2012. 2-D P–SV numerical study of soil–source interaction in a non-linear basin. *Geophys. J. Int.* (2012) 191, 1374–1390
- Gouedard, P., Stehly, L., Brenguier, F., Campillo, M., Colin de Verdiere, Y., Larose, E., Margerin, L., Roux, P., Sánchez-Sesma, F.J., Shapiro, N.M., Weaver, R. L., 2008. Cross-correlation of random fields: Mathematical approach and applications. *Geophysical prospecting*. 56(3), 375-393.
- Guéguen, P., Langlais, M., Foray, P., Rousseau, C., Maury, J., 2011. A natural seismic isolating system: The buried mangrove effects. *Bulletin of the Seismological Society of America*. 101(3), 1073-1080.
- Guéguen, P., 2016. Predicting nonlinear site response using spectral acceleration vs. PGV/Vs30: A case history using the Volvi-test site. *Pure and Applied Geophysics*, online first, doi [10.1007/s00024-015-1224-5](https://doi.org/10.1007/s00024-015-1224-5)
- Haddadi, H.R., Kawakami, H., 1998. Modeling wave propagation by using normalized input-output minimization (NIOM) method for multiple linear systems. *Structural Engineering Earthquake Engineering*. 15, 29s-40s.
- Hannemann, K., Papazachos, C., Ohrnberger, M., Savvaidis, A., Anthymidis, M., Lontsi, A.M., 2014. Three-dimensional shallow structure from high-frequency ambient noise tomography: New results for the Mygdonia basin-Euroseistest area, northern Greece. *Journal of Geophysical Research: Solid Earth*. 119(6), 4979-4999.

- Hardin, B.O., Black, W.L., 1968. Vibration modulus of normally consolidated clay. *Journal of Soil Mechanics and Foundations Division*. 94(2), 353-369.
- Haskell, N.A., 1953. The dispersion of surface waves on multilayered media. *Bulletin of the seismological Society of America*. 43(1), 17-34.
- Idriss, I.M., 2011. Use of V_{s30} to represent local site condition. Proc. 4th IASPEI/IAEE International Symposium. Effects of Source Geology on Seismic Motion. August 23-26th, 2011. University of Santa Barbara California.
- Johnson, P.A., Jia, X. P., 2005. Nonlinear dynamics, granular media and dynamic earthquake triggering. *Nature*. 437, 871-874.
- Kawakami, H., Haddadi, H.R., 1998. Modeling wave propagation by using normalized input-output minimization (NIOM). *Soil Dynamics and Earthquake Engineering*. 17(2), 117-126.
- Konno, K., and Ohmachi, T. 1998. Ground-motion characteristics estimated from spectral ratio between horizontal and vertical components of microtremor. *Bulletin of the Seismological Society of America*. 88(1), 228-241.
- Liu, P., Hartzell, S., Stephenson, W., 1995. Non-linear multiparameter inversion using a hybrid global search algorithm: applications in reflection seismology. *Geophysical Journal International*. 122(3), 991-1000.
- Lopez-Caballero, F., Razavi, A.M.F., Modaressi, H., 2007. Nonlinear numerical method for earthquake site response analysis I—elastoplastic cyclic model and parameter identification strategy. *Bulletin of Earthquake Engineering*. 5(3), 303-323.
- Mehta, K., Snieder, R., Graizer, V., 2007. Downhole receiver function: a case study. *Bulletin of the Seismological Society of America*. 97(5), 1396-1403.
- Miyazawa, M., Snieder, R., Venkataraman, A. 2008. Application of seismic interferometry to extract P-and S-wave propagation and observation of shear-wave splitting from noise data at Cold Lake, Alberta, Canada. *Geophysics*. 73(4), D35-D40.
- Modaressi, H., Foerster, E., 2000. *CyberQuake*. User's manual, BRGM, France.
- Mogi, H., Shrestha, S.M., Kawakami, H., Okamura, S., 2010. Nonlinear soil behavior observed at vertical array in the Kashiwazaki-Kariwa Nuclear Power Plant during the 2007 Niigata-ken Chuetsu-oki earthquake. *Bulletin of the Seismological Society of America*. 100(2), 762-775.
- Montoya-Noguera, S., Lopez-Caballero, F. 2016. Effect of coupling excess pore pressure

- and deformation on nonlinear seismic soil response. *Acta Geotechnica*. 11(1), 191-207.
- Nakata, N., Snieder, R., 2011. Near surface weakening in Japan after the 2011 Tohoku-Oki earthquake. *Geophysical Research Letters*. 38, L17302.
- Nakata, N., Snieder, R., 2012. Estimating near-surface wave velocities in Japan by applying seismic interferometry to KiK-net data. *Journal of Geophysical Research*. 117: B01308.
- Olsen, K.B., Day, S.M., Bradley, C.R., 2003. Estimation of Q for long-period (> 2 sec) waves in the Los Angeles basin. *Bulletin of the Seismological Society of America*. 93(2), 627-638.
- Parolai, S., Bindi, D., Ansal, A., Kurtulus, A., Strollo, A., Zschau, J., 2010. Determination of shallow S-wave attenuation by down-hole waveform deconvolution: A case study in Istanbul (Turkey). *Geophysical Journal International*. 181(2), 1147-1158.
- Pavlenko, O., Irikura, K., 2002. Changes in shear moduli of liquefied and nonliquefied soils during the 1995 Kobe earthquake and its aftershocks at three vertical-array sites. *Bulletin of the Seismological Society of America*. 92(5), 1952-1969.
- Pavlenko, O., Irikura, K., 2003. Estimation of nonlinear time-dependent soil behavior in strong ground motion based on vertical array data. *Pure and Applied Geophysics*. 160, 2365-2379.
- Péquegnat, C., Guéguen, P., Hatzfeld, D., Langlais, M., 2008. The French Accelerometric Network (RAP) and National Data Centre (RAP-NDC). *Seismological Research Letters*. 79(1), 79-89.
- Pilz, M., Parolai, S., Picozzi, M., Bindi, D., 2012. Three-dimensional shear wave velocity imaging by ambient seismic noise tomography. *Geophysical Journal International*. 189(1), 501-512.
- Rathje, E. M., Kottke, A. R., Trent, W. L., 2010. Influence of input motion and site property variabilities on seismic site response analysis. *Journal of geotechnical and geoenvironmental engineering*. 136(4), 607-619.
- Rathje, E. M., Chang, W. J., Stokoe, K. H., Cox, B. R., 2004. Evaluation of ground strain from in situ dynamic response. *Proceeding of the 13th World Conference on Earthquake Engineering, Vancouver, B.C., Canada, August 1-6, Paper No. 3099*
- Régnier, J., Cadet, H., Bonilla, L.F., Bertrand, E., Semblat, J.F., 2013. Assessing nonlinear

- behavior of soils in seismic site response: Statistical analysis on KiK-net strong-motion data. *Bulletin of the Seismological Society of America*. 103(3), 1750-1770.
- Rodriguez-Marek, A., Montalva, G.A., Cotton, F., Bonilla, F., 2011. Analysis of single-station standard deviation using the KiK-net data. *Bulletin of the Seismological Society of America*. 101(3), 1242-1258.
- Rubinstein, J.L, Beroza, G.C., 2004. Evidence for widespread nonlinear strong ground motion in the Mw 6,9 Loma Prieta earthquake. *Bulletin of the Seismological Society of America*. 94(5), 1595-1608.
- Rubinstein, J.L, Beroza, G.C., 2005. Depth constraints on nonlinear strong ground motion from the 2004 Parkfield earthquake. *Geophysical Research Letters*. 32, L14313.
- Satoh, T., Sato, T., Kawase, H. 1995. Nonlinear behavior of soil sediments identified by using borehole records observed at the Ashigra Valley, Japan. *Bulletin of the Seismological Society of America*. 85(6), 1821-1834.
- Satoh, T. 2006. Inversion of Qs of deep sediments from surface-to-borehole spectral ratios considering obliquely incident SH and SV waves. *Bulletin of the Seismological Society of America*. 96(3), 943-956.
- Sawazaki, K, Sato, H., Nakahara, H., Nishimura, T., 2009. Time-lapse changes of seismic velocity in the shallow ground caused by strong ground motion shock of the 2000 Western-Totori earthquake, Japan, as revealed from coda deconvolution analysis. *Bulletin of the Seismological Society of America*. 99(1), 352-366.
- Sens-Schönfelder, C., Wegler, U., 2006. Passive image interferometry and seasonal variations of seismic velocities at Merapi Volcano, Indonesia. *Geophysical research letters*. 33(21).
- Sleep, N.H., 2010. Nonlinear behavior of strong surface waves trapped in sedimentary basins. *Bulletin of the Seismological Society of America*. 100(2), 826-832.
- Snieder, R., Şafak, E., 2006. Extracting the building response using seismic interferometry: Theory and application to the Millikan Library in Pasadena, California. *Bulletin of the Seismological Society of America*. 96(2), 586-598.
- Thomson, W. T., 1950. Transmission of elastic waves through a stratified solid medium. *Journal of applied Physics*. 21(2), 89-93.
- Vucetic, M., 1994. Cyclic threshold shear strains in soils. *Journal of Geotechnical Engineering*. 120, 2208-2228.

Zeghal, M., Elgamal, A., Tang, H., Stepp, J., 1995. Lotung downhole array. II: Evaluation of soil nonlinear properties. *Journal of Geotechnical Engineering*. 121(4), 363–378.